Design and Testing of a Control System for Reverse-Flow Catalytic Afterburners

Miguel A. G. Hevia, Salvador Ordóñez, and Fernando V. Díez
Departamento de Ingeniería Química y Tecnología del Medio Ambiente, Universidad de Oviedo, Julián Clavería 8, 33006 Oviedo, Spain

Davide Fissore and Antonello A. Barresi
Dipartimento di Scienza dei Materiali ed Ingegneria Chimica, Politecnico di Torino, Corso Duca degli Abruzzi 24, 10129 Torino, Italy

DOI 10.1002/aic.10573
Published online August 11, 2005 in Wiley InterScience (www.interscience.wiley.com).

The design and testing of a control system for reverse-flow catalytic afterburners based on a two-variable bifurcation map is focused on. The combustion of lean methane–air mixtures is considered as the test reaction and a bench-scale apparatus, with a special temperature-control system based on dynamic compensation of the thermal losses to achieve adiabatic operation, is used for validation purposes. The aim of the control system is to avoid both catalyst overheating and reaction extinction when the adiabatic temperature increases and the flow rate of the feed changes. Stability maps of the reactor are obtained by means of numerical simulations, showing the values of the operating parameters (switching time), which allows fulfillment of the operating constraints (catalyst maximum temperature and methane conversion) when the inlet concentration and flow rate change. This system was realized and tested experimentally, mainly for inlet concentration changes, proving to be effective in all cases investigated. © 2005 American Institute of Chemical Engineers *AIChE J,* 51: 3020–3027, 2005
Keywords: reverse-flow reactors, autothermal combustion, reaction extinction, adiabatic reactor

Introduction

The reverse-flow catalytic reactor (RFR) is a device in which the feed flow direction is periodically reversed, thus giving rise to unsteady-state operation. When the combustion of cold and lean volatile organic compound (VOC) mixtures in air is carried out, the reversal of the flow direction traps the heat of reaction inside the bed, whose ending parts act as regenerative heat exchangers, thus allowing autothermal combustion and eliminating the need for auxiliary fuel to sustain the reaction. Extensive investigations about the RFR, including both numerical simulations and experimental analysis, were performed in the past 30 years and were reviewed, for example, by Matros and Bunimovich.[1]

In addition to the intrinsically dynamic behavior of the RFR, one must deal with unexpected external perturbations (in the feed concentration, composition, temperature, and flow rate), which may lead to reactor extinction (and thus later to reactant emissions) or catalyst overheating (and thus subsequent deactivation). To avoid these problems it is necessary to implement some closed-loop control strategy. Few papers have appeared in the literature concerning this topic. Van de Beld and Westerterp[2] discussed different possible solutions to avoid reactant emissions in a RFR in the case of temporary reduction of the concentration of the feed, but none of these proved to be effective:

(1) *Increasing of the feed temperature* requires a high energy input and, for control purposes, it is too slow because the entire bed has to be heated by the hotter feed.

Correspondence concerning this article should be addressed to A. A. Barresi at antonello.barresi@polito.it.

(2) *Adding combustibles to the feed* seems the most logical method to use because it is simple to implement, although a reactive combustible, when added to the feed, will already react in the inlet part of the catalyst bed and the increase of the maximum temperature in the center of the bed is initially small. Moreover, the ignition temperatures of the original pollutants and the supporting fuel must be almost equal; otherwise, the reactor may establish the temperature profile corresponding to the component with the lower ignition temperature and will not be able to oxidize the component with the higher ignition temperature.[3-5]

(3) *An electrical heating device in the center of the reactor* may increase the temperature in the hottest zone of the bed, even very rapidly, although the heat must be transferred from the heating device to the catalyst, thus introducing an additional heat transport resistance. Experimental results of Cunill et al.[6] show that this device is effective, given that the maximum temperature in the reactor is now a function of the electrical power and almost independent of the mixture components and composition; thus a mixture of contaminants with very different ignition temperatures can be burned completely, provided that the electrical power is sufficiently high. If a heating support is required for an extended period of time the electrical heating device may become too expensive; in this case, adding combustibles in the central part of the reactor is a better choice, even if lack of good distribution of the combustible over the entire cross-sectional area may cause difficulties.

(4) *Permanent addition of a component difficult to oxidize*, fed in a concentration sufficient to ensure the ignition, may be an alternative solution: the temperature level in the reactor will be high and all other less refractive contaminants will certainly be converted. The main drawback is that this is a rather energy-consuming solution; furthermore, an increase in the inlet concentration may be difficult to handle because the catalyst may become overheated.

(5) *Supply of a hot gas in the center of the reactor* is an inefficient way to increase the temperature because the heat capacity of the gas is low compared to that of the bed.

Finally, Barresi and Vanni[7] investigated the possibility of avoiding reaction extinction by acting on the switching time. They considered a one-point control strategy, with a temperature measurement located at either end of the active portion of the bed: flow direction is changed when temperature at the controller located close to the inlet drops below a certain set point. Their simulations provided evidence that at a higher set point the maximum temperature is also increased, although—at least for large portions of inert material—conversion cannot be arbitrarily improved by this strategy; this is explained by the shorter periods necessary for higher set points, resulting in a stronger washout effect. If the inlet concentration is lower than the minimum adiabatic temperature rise that is required to allow for autothermal operation, the change of the switching time may not be sufficient and the system evolves toward the extinction following a Zeno trajectory.[8]

Besides the problem of reaction extinction, the temperature in the reactor should not exceed the maximum allowable catalyst temperature, which may occur when the concentration of contaminants becomes too high during a significant period of time. A short peak of high concentration will not be a problem because the heat capacity of the system is high and it will take time before the maximum temperature exceeds the limit. Furthermore, the RFR exhibits some self-control with respect to the inlet concentration. For a low concentration, the reaction takes place in the central part of the reactor, so that part of the catalyst is used to store heat and to preheat the cold feed. If the inlet concentration is increased, the temperature and concentration profiles will move in the direction of the inlet and outlet of the reactor and a temperature plateau will develop. For higher inlet concentrations full conversion is already obtained in the first layers of the catalyst bed and the length of the "heat exchanger" equals that of the inert sections and remains constant. From this point, the maximum temperature will increase very rapidly with the inlet concentration. Different technical solutions have been proposed in the literature[9]:

(1) *Dilution of the feed with additional air* has the main drawback that the total flow rate increases significantly, thus requiring additional energy costs to overcome the higher pressure drop; moreover, there is the problem of obtaining reliable and inexpensive on-line measurements of the inlet concentration.[2]

(2) *Increase of the switching time* may lower the maximum temperature, particularly when high inert fraction is used.[3,6]

(3) *Heat recovery by internal heat exchange* was discussed by Grozev and Sapundzhiev[10] and by Nieken et al.,[3,4] who indicated that the switching period has to be increased, so that the reaction front approaches the center of the reactor before a noticeable influence on the maximum temperature can be noticed. However, no remarkable reduction of the maximum temperature is possible through intermediate cooling, irrespective of the switching period used, although the energy recovery increases. Sapundzhiev et al.[11] used an internal heat exchange to preheat the cold feed. External cooling restricts the region of operating variables that allows for autothermal behavior as combustion can now be quenched if the coolant removes more heat than is generated.[12]

(4) *Cold gas injection* into the middle of the packed bed may have an effect similar to that of intermediate cooling through heat exchange, leading to a significant decrease of the temperature in the middle of the reactor, whereas the maximum temperature is more or less unaffected.[4]

(5) *Hot gas withdrawal* from the center of the reactor allows for almost complete energy recovery, but again the maximum temperature cannot be lowered sufficiently: sidestream withdrawal just shifts the reaction zone toward the center of the reactor.[4]

(6) *Structured fixed bed.* If the packed bed is composed of portions with high effective conductivity and of portions of low conductivity then it depends on the position of the temperature fronts whether the maximum temperature is lowered or increased. If the fronts are always in the portion with high axial conductivity, the maximum temperature will be low and the efficiency of the heat recovery will be weak; if the fronts stay in the portion with low conductivity, the opposite is true. Because the position of the fronts can be shifted by the amount of the hot gas withdrawn, an interesting possibility exists to operate the reactor in either of the two regimes. To exploit this possibility a structured fixed bed is needed, where the packed bed is composed of three portions: an inner portion with high effective conductivity support and two outer portions with low conductivity support.[4]

Budman et al.[13] considered the application of a conventional PID controller with anti-windup: exit concentration, the controlled variable, is used to infer the maximum temperature (because thermocouple locations in the bed are fixed, it may be

extremely difficult to evaluate the maximum temperature, given that the temperature profiles move during the operation of the reaction). The same authors also considered a feedforward regulation of the exit concentration through knowledge of the inlet concentration. The idea behind this strategy is that if the inlet concentration is known, it is possible to evaluate the optimal combination of switching time and cooling rate to obtain full conversion and safe operation in the reactor. In this regard, a number of simulations have been performed to identify the parameters region for safe operation.

In this work a control system was used to control the reverse-flow operation in a catalytic afterburner: the switching time was varied to avoid both catalyst overheating and reaction extinction. By means of numerical simulations, a stability map of the reactor is obtained, showing the values of the switching time that allow fulfillment of the operating constraints (catalyst maximum temperature and methane conversion) when the inlet concentration and flow rate change.

To apply this control strategy we need to know both the inlet flow rate (which is easy to do and inexpensive) and the inlet concentration. Because on-line measurements may be difficult and expensive, a soft sensor based on high-gain techniques can be used to estimate the inlet concentration from some temperature measurements.[14]

The article is structured as follows: in Section 2 the detailed model used in the control system is described. In Section 3 the experimental apparatus is introduced and the mathematical model validated. In Section 4 the control algorithm is introduced and validated by means of simulations and of experiments.

The Model

A one-dimensional heterogeneous model was used to model the RFR. Pressure loss inside the system was neglected and plug flow, with dispersive transport of mass and energy, was assumed for the gas phase; the ideal gas law was used. The transient term was taken into account in the gas-phase equations as well as in the energy equation for the solid phase, whereas the solid catalytic surface was considered in pseudosteady-state condition. The effect of the intraparticle mass transport was included in the model by means of the effectiveness factor. The effect of the reactor wall on the thermal balance of the system is taken into account by means of a further energy balance equation for the wall. Thus, the dynamics of the adiabatic process can be described by the following set of partial differential-algebraic equations (PDAE):

Continuity Equation for the Gas Phase

$$\frac{\partial c_G}{\partial t} + \frac{\partial}{\partial x} c_G v = \sum_{i=1}^{n_r} \frac{k_{G,i} a_v}{\varepsilon} (y_{S,i} - y_{G,i}) \tag{1}$$

Continuity Equation for Component j in the Gas Phase

$$\frac{\partial y_{G,j}}{\partial t} = D_{eff} \frac{\partial^2 y_{G,j}}{\partial x^2} - v \frac{\partial y_{G,j}}{\partial x} + \frac{k_{G,j} a_v}{c_G \varepsilon} (y_{S,j} - y_{G,j}) - y_{G,j} \sum_{i=1}^{n_r} \frac{k_{G,i} a_v}{c_G \varepsilon} (y_{S,i} - y_{G,i}) \tag{2}$$

with $j = 1 \ldots (n_r - 1)$.

Energy Balance for the Gas Phase

$$\frac{\partial T_G}{\partial t} = \frac{k_{eff}}{\rho_G c_{p,G}} \frac{\partial^2 T_G}{\partial x^2} - v \frac{\partial T_G}{\partial x} + \frac{h a_v (T_S - T_G)}{\rho_G c_{p,G} \varepsilon} - \frac{4 h_i}{\rho_G c_{p,G} D_{R,i}} (T_G - T_W) \tag{3}$$

Mass Balance for the Solid Phase

$$k_{G,j} a_v (y_{S,j} - y_{G,j}) = [\rho_S (1 - \varepsilon)] \sum_{k=1}^{N_R} \eta_k \nu_{j,k} R'_{k,j} \tag{4}$$

with $j = 1 \ldots n_r$.

Energy Balance for the Solid Phase

$$\frac{\partial T_S}{\partial t} = \frac{\lambda_S}{\rho_S c_{p,S}} \frac{\partial^2 T_S}{\partial x^2} - \frac{h a_v}{\rho_S c_{p,S} (1 - \varepsilon)} (T_S - T_G) + \frac{1}{c_{p,S}} \sum_{i=1}^{n_r} \left(\sum_{k=1}^{N_R} \eta_k \nu_{i,k} R'_k \right) (-\Delta H_{f,i}) \tag{5}$$

Energy Balance for the Reactor Wall

$$\frac{\partial T_W}{\partial t} = \frac{\lambda_W}{c_{p,W} \rho_W} \frac{\partial^2 T_W}{\partial x^2} + \frac{4}{c_{p,W} \rho_W (D_{R,e}^2 - D_{R,i}^2)} D_{R,i} h_i (T_G - T_W) \tag{6}$$

Adiabatic operation is considered because the particular device adopted guarantees pseudoadiabatic behavior, as will be shown in the following. For the catalytic part of the reactor, a first-order rate equation was considered in the mass balance:

$$R'_{k,j} = k_r y_{S,j} = k_\infty \exp(-E_a / R T_S) y_{S,j} \tag{7}$$

$$k_\infty = k'_\infty \rho_S (1 - \varepsilon) R T_G \tag{8}$$

whereas for the inert sections the reaction rate was set equal to zero. Similarly, the solid physical properties—density, specific heat, and thermal conductivity—were set equal to the values either of the catalyst or of the inert sections, depending on the axial position in the reactor. If the physical and transport properties of the catalyst and of the inert sections are different, adequate boundary conditions (that is, identity in the heat and mass fluxes) must be specified at the boundary surface.

Conventional Danckwerts boundary conditions were assumed in $x = 0$ and $x = L$. Initially, the gas-phase temperature was considered constant along the reactor and equal to the inlet value, and the solid temperature was considered constant and equal to the preheating value.

Transport and dispersion parameters were evaluated according to previous works on the same subject.[15] Further details can be found in a previous publication.[16]

Table 1 shows the values of the main parameters and operating conditions used in the simulation of the RFR. The influ-

Table 1. Main Operating Parameters Considered in the Simulations of the RFR

Preheating temperature	650 K
Pellet diameter	2–4 mm
Catalyst density, ρ_S	2170 kg m^{-3}
Catalyst specific heat, $c_{p,S}$	848.1 J kg^{-1} K^{-1}
Catalyst porosity	0.519
Catalyst tortuosity	2
Catalyst thermal conductivity, λ_{eff}	0.472 W m^{-1} K^{-1}
Bed void fraction, ε	0.36
Frequency factor, k'_∞	1.0886×10^5 mol kg^{-1} s^{-1} Pa^{-1}
Activation energy, E_{att}	1.12504×10^5 J mol^{-1}
Inlet gas temperature	298 K

ence of the temperature and composition on the density and on the specific heat of the gas was taken into account.

The domain of the spatial variable x was discretized on a grid of equally spaced points; 101 points are enough to ensure a grid-independent solution. As a consequence, the PDAE system (Eqs. 1–6) was transformed into a differential algebraic equations (DAE) problem. The integration in time of the differential part of the system was performed by implementing the Fortran routine LSODES, from the package ODEPACK.[17] Both relative and absolute tolerance were set to the square root of the working machine precision.

After a transient period, the solution of the system evolves toward a pseudosteady state (PSS), given that the behavior of the reactor (temperature and concentration profiles) is the same within every cycle.

The Bench-Scale Rig and Model Validation

The design of the experimental reactor to carry out the model validation (and subsequent test of the control system) was mainly aimed to reproduce as fairly as possible the behavior of large-scale industrial reactors. The major drawback found when working on the fulfillment of this goal, apart from the influence of the wall thermal inertia that is taken into account in our model, is the difficulty in obtaining operation regimes close to adiabaticity with small-sized reactors. This is because the higher ratio of external surface to volume, which is characteristic of small reactors (low diameters), causes the heat losses to be relatively more important with regard to the overall thermal balance of the system. Thus, whereas in large-industrial reactors adiabatic behavior can be assumed, it is not possible to do the same with small lab-scale or even pilot-scale reactors and it is necessary to use heat-transfer coefficients to take into account the heat losses.[18,19]

In this work, this problem is solved using a special device with its own control system, which acts over the temperature outside the reactor. Such a control system is able to cause such outer temperature to dynamically follow the axial inner temperature in every axial position, thus eliminating the driving force to the heat transmission in the radial direction, and therefore the heat losses. Because axial temperature profiles are not uniform and change with time as a consequence of unsteady-state operation, the heating system was divided into seven sections or band heaters, each of them independently controlled by different PID controllers. The central band heater is 0.10 m long and the others are 0.065 m long: this was the best compromise between efficiency and complexity of the device. To follow the dynamic of the temperature in the reactor, cooling air has to be supplied to cool down reactor surroundings when the bed temperature decreases, thus avoiding further heating arising from the thermal inertia of the band heater. This system is currently undergoing a patent application[20] and has been described in detail in a previous paper.[16]

The reactor is a 316 stainless steel tube with 0.496 m effective (filled with packing) length, an inner diameter of 5.17×10^{-2} m, and a wall reactor thickness of 1.15×10^{-3} m. The packing includes catalyst and inert material. The latter consists of two sections of glass spheres (4×10^{-3} m diameter) at both ends of the bed, each one taking up 24.8% of the effective length. A commercial catalyst was used composed of a mixture of metal oxides supported on γ-alumina, forming spheres with an average diameter of 4×10^{-3} m. The kinetics of methane combustion over this catalyst was studied in an isothermal fixed-bed reactor,[21] from which it was determined that a pseudo-first-order law accurately fitted the results. Analysis of the gas streams was carried out by means of an HP 6890 GC equipped with an HP-5 capillary column and flame ionization detector (FID).

Several experiments were carried out, changing the values of the main operating parameters, such as switching time, inlet concentration, and surface gas velocity to test the adequacy of the model to simulate the behavior of the reactor. Figure 1 shows an example of the solid temperature profiles obtained for various values of the operating parameters—switching time, inlet concentration, and surface gas velocity—when the PSS has been reached (the temperature profiles at the middle of a semicycle are shown). The experimental values are compared to those obtained by simulation of the adiabatic reactor, also proving that the dynamic compensation of the heat losses is effective in achieving adiabatic operation and avoiding overcompensation. The agreement between the experimental measured values of the temperature and the simulated values is fairly good. It is important to highlight that no fitting parameters were used in the simulation of the reactor so that the model can be considered fully predictive.

The Control Algorithm

By means of numerical simulation a stability map of the reactor can be obtained that delimits regions where maximum temperature (or conversion) is higher or lower than a certain value. The full map is a function of three parameters: the switching time (which will be the manipulated variable) and the inlet concentration and surface velocity (which are the disturbances). Figure 2 (top graph) shows a section of this map, obtained with a value of the surface velocity of the gas equal to 0.14 m s^{-1}, whereas Figure 2 (bottom graph) shows a section of the map, obtained with a value of the inlet concentration equal to 4000 ppmV. Because of process constraints on outlet reactant conversion and maximum temperature on the solid, a well-defined operating region is obtained as a function of the three parameters: the disturbances and the manipulated variable. In both sections of the stability map shown in Figure 2 the region corresponding to methane conversion $> 99.95\%$ and maximum solid temperatures < 650°C is evidenced. In the definition of the operating region it is also possible to take into account modeling errors by defining a percentage uncertainty over these curves.

Until the point corresponding to the operating conditions (inlet concentration, inlet surface velocity, and switching pe-

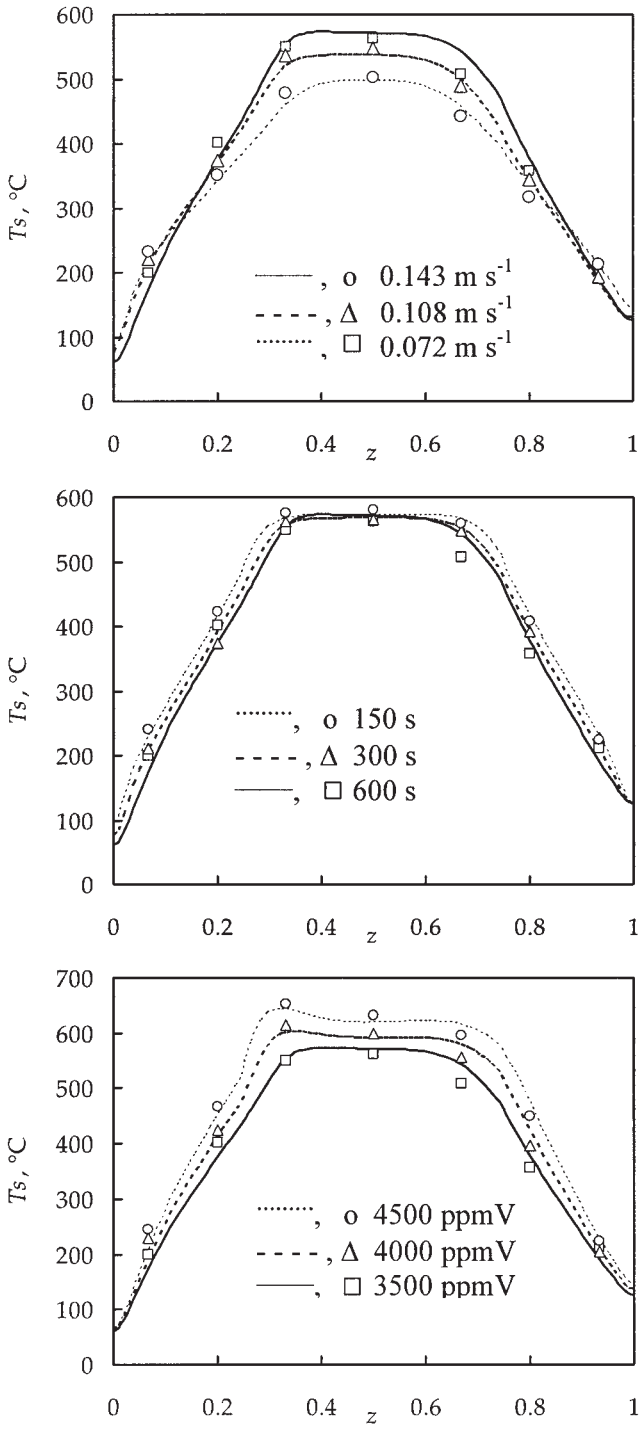

Figure 1. Simulated (lines) axial temperature profiles and actual measurements (symbols) in the middle of a cycle, when the PSS was reached, for various values of the switching time (graph A, $u_{G,0} = 0.143$ m s^{-1}, $y_{CH4,0} = 3500$ ppmV), gas velocity (graph B, $y_{CH4,0} = 3500$ ppmV, $t_c = 600$ s), and inlet methane concentration (graph C, $u_{G,0} = 0.143$ m s^{-1}, $t_c = 600$ s).

riod) is in the optimal region no control action is taken; if the inlet concentration increases too much, as well as if the inlet surface velocity increases too much, the control system has two possibilities: it may increase the switching time (because the maximum temperature decreases slightly when the switching time is increased) or, if this is not sufficient, it may dilute the feed to remain in the optimal working region. If the inlet concentration decreases too much, as well as if the inlet surface velocity decreases, a control action is taken just when the outlet conversion starts decreasing (because of the thermal inertia of the system, the reactor is able to sustain periods of low inlet concentration, with no decrease in the outlet conversion): either the switching time is reduced, if this can increase the conversion, or auxiliary fuel is added when the inlet concentration, or the inlet surface velocity, is lower than the minimum value that allows adiabatic operation.

In the example considered in Figure 3 (top graph) a reduction of the switching time is sufficient to avoid any conversion decrease (bottom graph) after the reduction in the methane concentration of the feed. The subsequent increase in the inlet

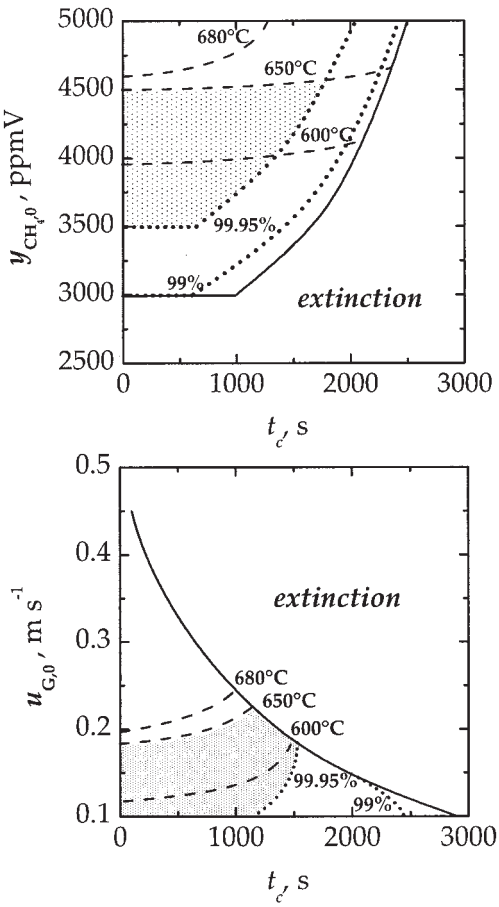

Figure 2. Example of stability map of a RFR (top graph: $u_{G,0} = 0.14$ m s^{-1}; bottom graph: $y_{CH4,0} = 4000$ ppmV).

The solid line separates the region where extinction occurs from the region where stable operation can be obtained; dotted lines separate the regions where conversion is larger (top part) or lower than the specified value; dashed lines separate the regions where maximum solid temperature is higher (top part) or lower than the specified value.

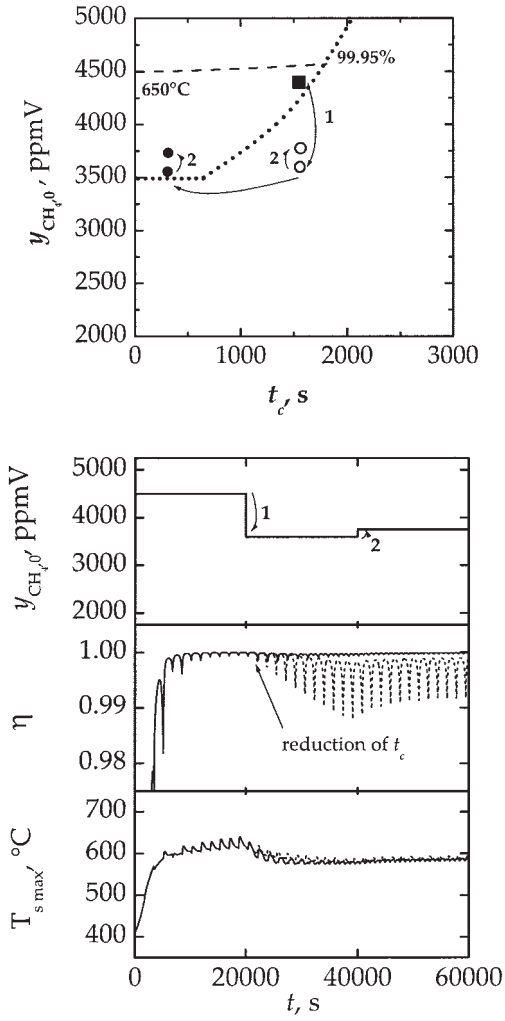

Figure 3. Bottom graph: maximum solid temperature and outlet methane conversion in a RFR when the inlet concentration is varied according to the top graph.

Variation of the switching time is considered to maintain the system in the optimal region. The behavior with (solid line) and without (dashed line) control action is compared. Disturbance and control action are evidenced on the stability map (top graph).

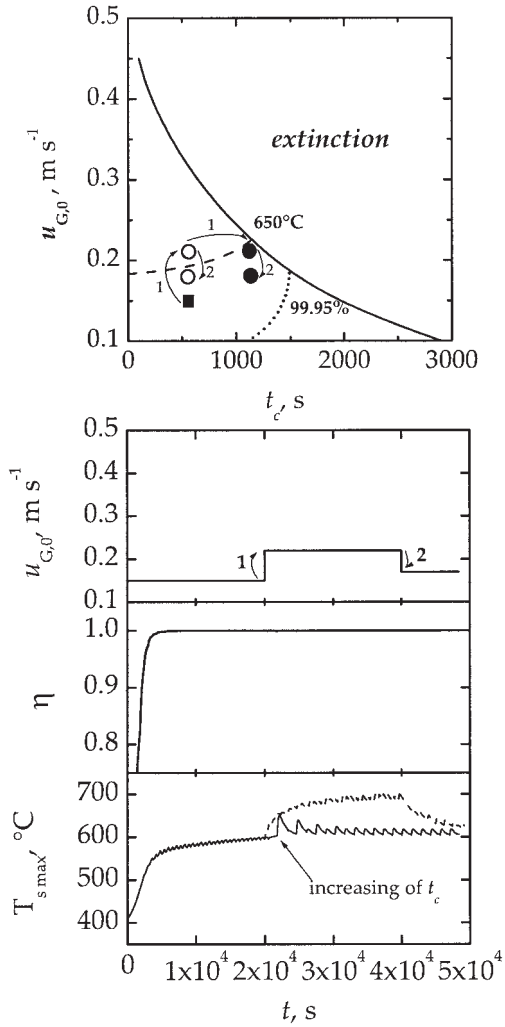

Figure 4. Bottom graph: maximum solid temperature and outlet methane conversion in a RFR when the inlet surface velocity is varied according to the top graph.

Variation of the switching time is considered to maintain the system in the optimal region. The behavior with (solid line) and without (dashed line) control action is compared. Disturbance and control action are evidenced on the stability map (top graph).

concentration does not require any control action as the system remains in the optimal working region. In the example considered in Figure 4 (top graph) the switching time in increased to face against the catalyst overheating resulting from the increase of the surface velocity (bottom graph). It is important to stress that this control system based on the model of the process is able to avoid any control action when this is useless and it is able to fulfill any constraints on process operation, being sufficient to indicate them in the working map.

The performance of the control system was also experimentally tested. The requirements considered were 1 ppmV for the semicycle averaged outlet concentration, and 650 °C for the maximum temperature, which was experimentally demonstrated to be the maximum temperature that the catalyst can endure without deactivation. The changes of the inlet concentrations, the times at which they were introduced, and responses of the control system are included in Table 2. The negative perturbations of the inlet concentration endanger the stability of the reactor and can lead to an increase of the outlet concentration and, eventually, to the extinction. By contrast, the risk of positive perturbations is

Table 2. Perturbations, Time at Which They Were Introduced, and Responses of the Control System

	Perturbation	Perturbation
$y_{G,0} \times 10^6$ initial	3500	3500
$y_{G,0} \times 10^6$ final	3050	3950
t, perturbation*	9900s	4400s
t_c initial	990s	120s
t_c final	150s	990s

*Time elapsed from the beginning of the experiment to the perturbation.

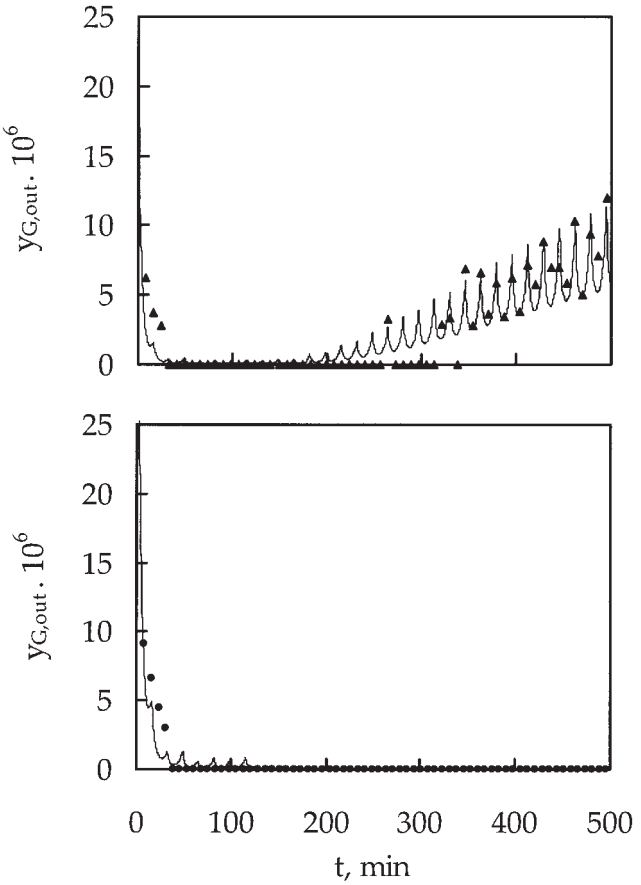

Figure 5. Experimental test of the performance of the control system for a negative inlet concentration perturbation (see Table 2).

Comparison between experimental value of the outlet methane concentration (symbols) and simulated values (lines) when no control action is undertaken (top graph) and when the control system is working (bottom graph).

the overheating. This is why the interesting variable to follow in the former case is the outlet concentration, whereas in the latter one is the maximum temperature.

Four experimental runs, with and without applying the control system for a negative and a positive perturbation, were carried out, and the control system performed as theoretically expected for both types of disturbances in all cases. Figure 5 shows the concordance with the corresponding simulated results. Moreover, in this figure it can be observed that the outlet concentration in the uncontrolled response increases with time, whereas in the controlled one tends to zero. In this way, the diminution of the switching time is in practice demonstrated to be an effective measure to avoid the outlet concentration increase that takes place as a consequence of a negative perturbation.

The results for a positive perturbation are shown in Figure 6, pointing out that, although instant maxima appear in the controlled response in the first minutes after the perturbation, the control system eventually dampens the temperature increase, otherwise occurring in the uncontrolled response.

Conclusions

A control system based on a detailed model was designed for a catalytic afterburner. A detailed one-dimensional model was used to simulate the operation in a bench-scale reactor with an innovative system for compensation of thermal losses. The control strategy, based on the appropriate choice of the switching time according to the operating conditions (inlet gas velocity, concentration), was demonstrated to be effective in preventing both catalyst overheating and reaction extinction (and thus reactant emissions), avoiding any control action when this is useless, even if the inlet flow rate and concentration changes, but remaining in the optimal working region. When acting on the switching time is not sufficient, maximum temperature is decreased by dilution of the feed, which has proved to be the simplest and more effective control action to achieve the desired result and unitary conversion is guaranteed by injection of auxiliary fuel. The pumping costs associated with the air dilution and those attributed to the auxiliary fuel, which also generates additional carbon dioxide emissions, are reduced because this measure will be adopted just when large perturbations occur.

To apply this control strategy we need to know both the inlet flow rate (which is easy to do and inexpensive) and the inlet concentration. Because on-line measurements may be difficult

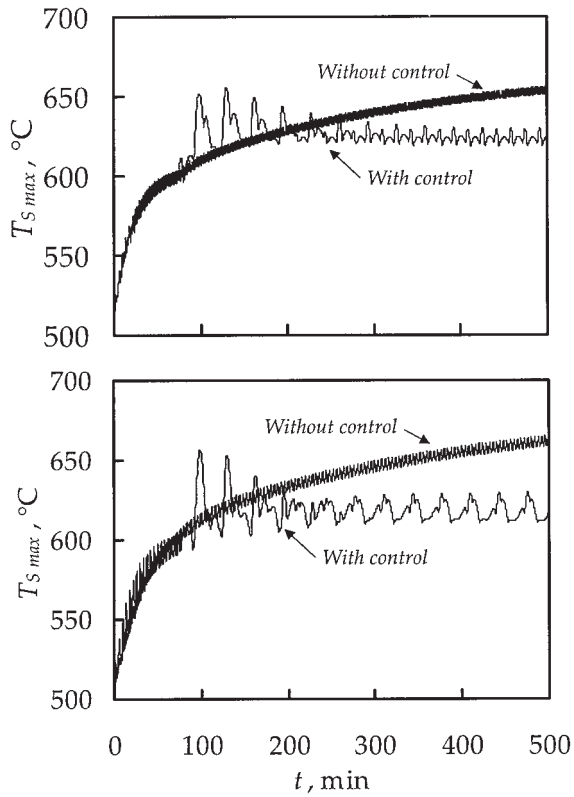

Figure 6. Comparison between the simulated (top graph) and the experimental values (bottom graph) of the maximum temperature (among the seven axial positions in which the temperature is measured) of the reactor to a positive inlet concentration perturbation (see Table 2) with and without control system.

and expensive, a soft sensor based on high-gain techniques can be used to estimate the inlet concentration from some temperature measurements.

Acknowledgments

This work was financially supported by the European Community (Contract ENV4-CT97-0599). The financial support of Italian and Spanish Ministries of University and Research (Project "Integrated Actions Italy–Spain") is also gratefully acknowledged.

Notation

a_v = external particle surface area per unit volume of reactor, m^{-1}
c = molar concentration, mol m^{-3}
c_p = specific heat at constant pressure, J kg^{-1} K^{-1}
D_{eff} = effective mass dispersion coefficient, m^2 s^{-1}
d_P = pellet diameter, m
D_R = reactor diameter, m
E_a = activation energy, J $kmol^{-1}$
ΔH_f = molar enthalpy of formation, J mol^{-1}
h = gas-solid heat transfer coefficient, J m^{-2} K^{-1} s^{-1}
k_∞ = preexponential factor, s^{-1}
k'_∞ = frequency factor, mol kg^{-1} s^{-1} Pa^{-1}
k_{eff} = effective heat dispersion coefficient, J m^{-1} K^{-1} s^{-1}
k_G = gas–solid mass transfer coefficient, mol m^{-2} s^{-1}
k_r = kinetic constant, s^{-1}
L = total reactor length, m
N_R = number of reactions
n_r = number of components in the mixture
Pr = Prandt number
R = ideal gas constant, J K^{-1} mol^{-1}
R' = reaction rate, s^{-1}
Re_P = particle Reynolds number
Sc = Schmidt number
T = temperature, K
t = time, s
t_c = switching time, s
u = surface velocity, m s^{-1}
v = interstitial velocity, m s^{-1}
x = axial reactor coordinate, m
y = molar fraction
z = nondimensional axial reactor coordinate, $z = x/L$

Greek letters

ε = bed void fraction
η = effectiveness factor
λ = thermal conductivity, J m^{-1} K^{-1} s^{-1}
λ_{st} = thermal conductivity of the stagnant gas, J m^{-1} K^{-1} s^{-1}
ν = stoichiometric coefficient
ρ = density (or apparent density for the solid), kg m^{-3}

Subscripts and superscripts

0 = inlet conditions
e = external value
G = gas phase
i = internal value
max = maximum value
S = solid phase or solid surface
W = reactor wall

Abbreviations

RFR = reverse-flow reactor
PSS = periodic steady state

Literature Cited

1. Matros YS, Bunimovich GA. Reverse-flow operation in catalytic reactors. *Catal Rev Sci Eng.* 1996;38:1-68.
2. Van de Beld L, Westerterp KR. Operation of a catalytic reverse flow reactor for the purification of air contaminated with volatile organic compounds. *Can J Chem Eng.* 1997;75:975-983.
3. Nieken U, Kolios G, Eigenberger GA. Fixed-bed reactors with periodic flow reversal: Experimental results for catalytic combustion. *Catal Today.* 1994;20:335-350.
4. Nieken U, Kolios G, Eigenberger GA. Control of the ignited steady state in autothermal fixed-bed reactors for catalytic combustion. *Chem Eng Sci.* 1994;49:5507-5518.
5. Cittadini M, Vanni M, Barresi AA, Baldi G. Development and design of a forced unsteady-state reactor through numerical simulation. In: *Proceedings of the 10th European Symposium on Computer Aided Process Engineering* (Computer-Aided Chemical Engineering Series). Vol. 8. Amsterdam: Elsevier; 2000:697-702.
6. Cunill F, Van de Beld L, Westerterp KR. Catalytic combustion of very lean mixtures in a reverse flow reactor using an internal electrical heater. *Ind Eng Chem Res.* 1997;36:4198-4206.
7. Barresi AA, Vanni M. Control of catalytic combustors with periodical flow reversal. *AIChE J.* 2002;48:648-652.
8. Mancusi E, Russo L, di Bernardo M, Crescitelli S. Zeno trajectories in a non-smooth model of a controlled reverse flow reactors. Proc of European Symposium on Computer-Aided Chemical Engineering (ESCAPE-14), Lisbon, Portugal, May 19–23; 2004.
9. Eigenberger G, Nieken U. Catalytic combustion with periodical flow reversal. *Chem Eng Sci.* 1988;43:2109-2115.
10. Grozev GG, Sapundzhiev CG. Modelling of reversed flow fixed bed reactor for catalytic decontamination of waste gases. *Chem Eng Technol.* 1997;20:378-383.
11. Sapundzhiev C, Chaouki J, Guy C, Klvana D. Catalytic combustion of natural gas in a fixed bed reactor with flow reversal. *Chem Eng Commun.* 1993;125:171-186.
12. Purwono S, Budman H, Hudgins RR, Silveston PL, Matros YS. Runaway in packed bed reactors operating with periodic flow reversal. *Chem Eng Sci.* 1994;49:5473-5487.
13. Budman H, Kzyonsek M, Silveston P. Control of nonadiabatic packed bed reactor under periodic flow reversal. *Can J Chem Eng.* 1996;74:751-759.
14. Edouard D, Schweich D, Hammouri H. Observer design for reverse-flow reactor. *AIChE J.* 2004;50:2155-2166.
15. Van de Beld L. *Air Purification by Catalytic Oxidation in an Adiabatic Packed Bed Reactor with Periodic Flow Reversal*. PhD Thesis. Enschede, The Netherlands: University of Twente; 1995.
16. Fissore D, Barresi AA, Baldi G, Hevia MAG, Ordóñez S, Díez F. Design and testing of small scale unsteady-state afterburners and reactors. *AIChE J*. 2005;51:1654-1664.
17. Hindmarsh AC. *ODEPACK, A Systematized Collection of ODE Solvers*. Stepleman RS, et al., eds. (Vol. 1 of IMACS Transactions on Scientific Computation). Amsterdam: North-Holland; 1983.
18. Van de Beld L, Borman RA, Deckx OR, Van Woezik BAA, Westerterp KR. Removal of volatile organic compounds from polluted air in a reverse flow reactor: An experimental study. *Ind Eng Chem Res.* 1994;33:2946-2956.
19. Ben-Tullilah M, Alajem E, Sheintuch M. Flow-rate effects in flow reversal reactors: Experiments, simulations, approximations. *Chem Eng Sci.* 2003;58:1135-1146.
20. Díez F, Vega A, Ordóñez S, Hevia MAG, Fissore D, Cittadini M, Vanni M, Barresi AA, Baldi G. *Dispositivo para el control de flujo de calor a través de la pared en equipos pequeños*. Spanish Patent Application No. P200400625; 2004.
21. Hurtado P, Ordóñez S, Vega A, Díez FV. Methane catalytic combustion over commercial catalysts in presence of ammonia and hydrogen sulphide. *Chemosphere.* 2004;65:681-689.

Manuscript received Sep. 9, 2004, revision received Feb. 18, 2005, and final revision received Apr. 26, 2005.